American Journal of Pathology, Vol. 145, No. 1, July 1994

Bcl-2 Protein Expression During Murine Development

Deborah Veis Novack and
Stanley J. Korsmeyer

From the Departments of Medicine and Pathology, Howard Hughes Medical Institute, Washington University School of Medicine, St. Louis, Missouri

Bcl-2 functions as a death repressor molecule in an evolutionarily conserved cell death pathway. To further explore the role of Bcl-2 in development, we assessed its pattern of expression during murine embryogenesis. Immunohistochemical analysis demonstrates that Bcl-2 is widely expressed early in mouse fetal development in tissues derived from all three germ layers and that this expression becomes restricted with maturation. Within epithelium, the E12.5 lung bud demonstrates a proximal to distal gradient of Bcl-2 expression which is enhanced by E18.5. Bcl-2 is expressed throughout the intestinal epithelium through E14.5, but by E18.5 only cells in the crypts and lower villi express Bcl-2. In the mesoderm-derived kidney, Bcl-2 is expressed in both the ureteric bud and metanephric cap tissue at E12.5. Tubular structures also express Bcl-2, although overall levels drop as the kidney matures. Retinal neuroepithelial cells uniformly express Bcl-2 until cells begin to differentiate and then display the topographic distribution maintained into adulthood. The developing limb provides a clear example where Bcl-2 is restricted to zones of cell survival; Bcl-2 is expressed in the digital zones but not in the interdigital zones of cell death. The wide distribution of Bcl-2 in the developing mouse suggests that many immature cells require a death repressor molecule or that Bcl-2 may have roles beyond regulating developmental cell death. (Am J Pathol 1994, 145:61–73)

Bcl-2 is translocated into the Ig locus and overexpressed in the majority of follicular B cell lymphomas[1–3] and is oncogenic when overexpressed in transgenic mice within B cells.[4] *Bcl-2* is unique among oncogenes because it exerts its oncogenic effect via the inhibition of apoptosis and not via enhanced cell cycle progression.[4,5] A variety of *in vitro* and *in vivo* model systems have shown that overexpressed *Bcl-2* can increase survival when cells are exposed to many but not all apoptotic stimuli. For example, *Bcl-2* prevents death of hematopoietic cell lines after withdrawal of interleukin-3, interleukin-4, and granulocyte macrophage colony-stimulating factor, but not interleukin-2 or interleukin-6.[6,7] In transgenic mice that express *Bcl-2* in immature thymocytes, these cells are resistant to glucocorticoid, anti-CD3, and γ-irradiation treatments but still undergo negative selection.[8,9] The expression of *Bcl-2* in long-lived and progenitor cells within adult tissues[10] supports the hypothesis that the role of *Bcl-2* in normal tissues is to enhance cell survival. During lymphocyte differentiation, low levels of *Bcl-2* correlate with increased susceptibility to apoptosis.[11,12] Thymocytes from *Bcl-2*-deficient mice differentiate normally but become depleted with age; *in vitro*, thymocytes undergo accelerated death with exposure to apoptotic stimuli.[13] This mouse model demonstrates that *Bcl-2* is an important regulator of cell survival *in vivo*.

Bcl-2 is a 25-kd integral membrane protein that has been localized to mitochondria, nuclear envelope/perinuclear membrane, and endoplasmic reticulum.[14–18] Although its precise biochemical role remains uncertain, *Bcl-2* appears to function in an antioxidant pathway. Expression of *Bcl-2* within hematopoietic cell lines prevented death in response to oxidative stresses including hydrogen peroxide and menadione.[19] In this system, *Bcl-2* did not alter the generation of reactive oxygen species but prevented damage to cellular constituents, including lipid peroxidation. *Bcl-2* expression also blocked

Supported in part by NIH grant CA 49712. DVN was supported by NIH training grant 5 T32 EY07108.

Accepted for publication March 10, 1994.

Address reprint requests to Dr. Stanley J. Korsmeyer, Howard Hughes Medical Institute at Washington University School of Medicine, Box 8022, 660 South Euclid, St. Louis, MO 63110.

necrotic cell death following glutathione depletion in a hippocampal cell line.[20] *Bcl-2* expressing cells demonstrated decreased peroxides and decreased lipid peroxidation after this stimulus.

Cell death is a common event during the fetal and early postnatal development of many tissues.[21] For example, cell death is an important component of the modeling of the digits in the limb bud. An unresolved developmental question is how a cell knows whether it should survive or self-destruct. Determining the expression of proteins which regulate cell survival is a critical aspect to understanding this process.

Bcl-2 has been shown to prevent programmed cell death induced by a wide array of signals. This suggests that *Bcl-2* is a central repressor of cell death that might have an important regulatory role during the development of many organs. Prior studies of *Bcl-2* in human fetal tissue suggested that its expression was more widespread in the embryo than in the adult.[22] Consequently, we used a monoclonal antibody to perform an extensive survey of the pattern of *Bcl-2* expression during critical periods of murine embryonic development.

Materials and Methods

Animals

C3H×C57BL/6 F_1 mice were purchased from Taconic Farms (Germantown, NY). Females were superovulated with pregnant mare serum and human chorionic gonadotropin (Sigma Chemical Co., St. Louis, MO). Matings were performed overnight in our own facilities. The morning on which vaginal plugs were observed was considered to be E0.5. The morning on which pups were observed was considered to be P0.

Western Blot Analysis

Western blot analysis was performed as described.[11] Hamster monoclonal antibodies 3F11 (anti-mouse *Bcl-2*)[11] and TN3 (anti-human tumor necrosis factor-α, a gift from Dr. R. Schreiber) were purified from hybridoma supernatants on protein A-Sepharose. Rat monoclonal antibody 4C11 (anti-mouse *Bcl-2*, a gift from Dr. G. Nunez) was purified from hybridoma supernatant on protein G-Sepharose. Polyclonal rabbit serum bc1 (anti-cytochrome b1) was a gift from Dr. J. Hare. Mouse monoclonal antibody 3C1–1 (anti-histone H3) was a gift from Dr. J. Portanova, Monsanto Corp.

Immunohistochemistry

Immunoperoxidase staining was performed using the hamster monoclonal antibodies 3F11 and TN3 exactly as described.[11]

Subcellular Fractionation

Whole brains were removed from E16.5 mice and forced through nylon mesh in hypotonic buffer (42.5 mmol/L KCl, 10 mmol/L HEPES, pH 8.0, 5 mmol/L $MgCl_2$), then lysed with a dounce four times with a pestle; this preparation was called the total lysate. The total lysate was diluted 1:1 with isolation buffer (0.32 mol/L sucrose, 1 mmol/L EGTA pH 8.0, 3 mmol/L $MgCl_2$, 10 mmol/L HEPES pH 8.0) and spun at 200 × *g* for 5 minutes at 4 C. The resulting pellet was washed once in isolation buffer with 0.2% Triton X-100, resuspended in isolation buffer with 0.2% Triton X-100, and mixed with 6.25 volumes of 2.39 mol/L sucrose. This sucrose mixture was spun at 60,000 × *g* for 1 hour at 4 C; the resulting nuclear pellet was washed once in isolation buffer and then resuspended in a small volume of isolation buffer. The supernatant from the original 200 × *g* spin was spun again at 200 × *g* to remove residual nuclei, then spun at 3100 × *g* for 10 minutes. The 3100 × *g* pellet was resuspended in isolation buffer, loaded over 25% Percoll (Sigma), and spun at 60,000 × *g* for 1 hour at 4 C. The heavy membrane fraction appeared as a white fluffy band approximately 2 cm from the top of the Percoll gradient; this band was aspirated, washed once in isolation buffer, and resuspended in a small volume of isolation buffer. The supernatant from the first 3100 × *g* spin was spun again at 3100 × *g*, then spun at 150,000 × *g* to separate light membranes (pellet) from cytosol (supernatant). The cytosol fraction was concentrated fourfold with a Centriprep 10 (Amicon, Beverly, MA). All fractions were quantitated with the D/C protein assay kit (Bio-Rad, Hercules, CA), and 50 µg were loaded in each lane. All solutions contained the protease inhibitors aprotinin and phenylmethylsulfonyl fluoride.

Results

Antibody Specificity

To study the distribution of *Bcl-2* during development, the hamster anti-mouse *Bcl-2* antibody (Ab) 3F11 was raised.[11] This Ab sees a 25-kd band on Western analysis of the murine pro-B cell line FL5.12 (Figure 1, lane 1) and in a human T cell line CEM-C7 stably transfected with a murine *Bcl-2* expression vector

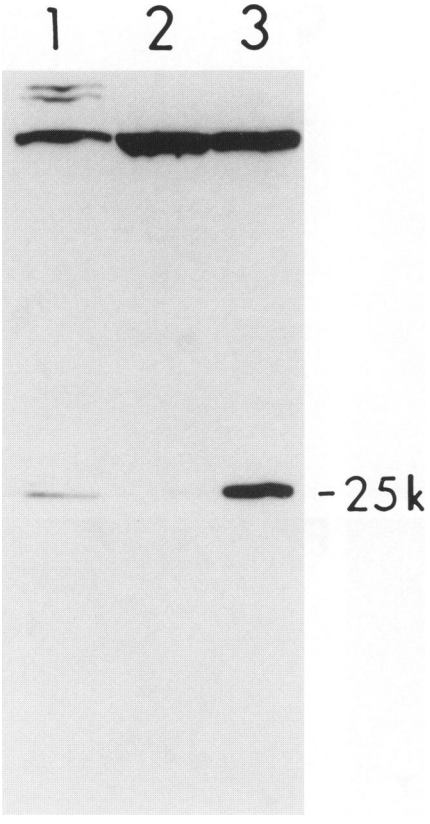

Figure 1. *3F11 recognizes 25-kd murine Bcl-2. Western analysis of lysates from 10^6 cells from the murine cell line FL5.12* (lane 1), *the human parent cell line CEM-C7* (lane 2), *and the mBcl-2 transfectant CMB8* (lane 3) *hybridized with 3F11 (hamster anti-mouse Bcl-2). CEM-C7 was transfected with mBcl-2 cDNA in pSSFVNeo[7] to generate the stable clone CMB8. The high molecular weight bands are not specific to the 3F11 Ab, since they are seen with the goat anti-hamster Ab alone.*

(lane 3). It does not recognize the human *Bcl-2* protein expressed in CEM-C7 (lane 2) or in human thymus.[11]

Distribution of Bcl-*2 Protein in Whole Embryo Sections*

To perform a broad survey of *Bcl-2* expression, embryos from 10.5 to 18.5 days' gestation (E10.5 to E18.5) were sectioned parasagittally and stained with the anti-*Bcl-2* monoclonal antibody 3F11. *Bcl-2* expression was also noted at E8.5, the earliest time point examined (not shown). At E10.5 (Figure 2B), the most prominent *Bcl-2* expression was found in the immature neural tissue of the brain (closed arrowhead) and spinal cord (wide arrow). *Bcl-2* protein could also be seen in the first branchial arch (curved arrow), gut (thin arrow), and somites (open arrowhead), but was notably absent from loose connective tissue areas.

At E12.5 (Figure 2C), *Bcl-2* expressing cells were found in the forebrain (large arrowhead), midbrain (not shown), and hindbrain (small arrowhead), as well as in dorsal root ganglia (large arrow). *Bcl-2* expression was also substantial in developing lung (curved arrow), gut (open arrowhead), and kidney (thin arrow), but was noticeably lower in the liver and in the connective tissues of the head and body.

At E14.5 (Figure 2D), *Bcl-2* expression was very widespread and intense, but not ubiquitous. The brain had differentiated extensively by this time, and *Bcl-2* expression was no longer as uniform as in the undifferentiated neuroepithelium of earlier embryos. *Bcl-2* expression was highest in the cortical plate (large arrowhead), a population of postmitotic neurons which contributes to the mature cortex. *Bcl-2* was also found in the proliferative zones adjacent to the ventricles and in the pituitary (small arrowhead). However, *Bcl-2* staining was absent from the densely packed thalamus (wide arrow). Outside the nervous system, the overall pattern of *Bcl-2* expression was similar to that at E12.5; *Bcl-2* was identified in the gut (open arrowhead) but not the liver (open arrow). Whisker follicles (curved arrow) and hindlimb also demonstrated *Bcl-2* staining.

At E16.5 (Figure 2E), the distribution of *Bcl-2* protein had not changed dramatically from E14.5. Spinal cord (arrowhead) maintained *Bcl-2* protein despite a high incidence of developmental cell death at this time. In the kidney (thin arrow), there appeared to be a gradient of *Bcl-2* protein, with the highest levels found in the immature cap tissue near the surface. The lung also demonstrated heterogeneous staining (curved arrow). Hair follicles also expressed *Bcl-2*, although intense surface staining of the skin was artifactual. At E18.5 (Figure 2F), *Bcl-2* expression in the brain was still prominent, but overall staining intensity in the cortical plate (large arrowhead) decreased as the cells in this layer differentiated. Staining was still intense in the nasal epithelium. In the oral cavity, *Bcl-2* was found in the epithelial surface of the tongue and in the ameloblasts and odontoblasts of the incisor bud (wide arrow). *Bcl-2* was also identified in the thymus (curved arrow). Staining in the brown fat deposits (small arrowhead) and bladder (long arrow) was artifactual. The overall level of *Bcl-2* expression had noticeably decreased relative to E14.5-E16.5.

*Subcellular Localization of m*Bcl-*2*

Examination of embryo sections at high magnification revealed *Bcl-2* staining throughout most cells over both the nucleus and cytoplasm. The cortical plate of the brain at E14.5 to E16.5 displayed intense staining and was therefore chosen for further localization studies. Figure 3A shows the typical pattern of staining by

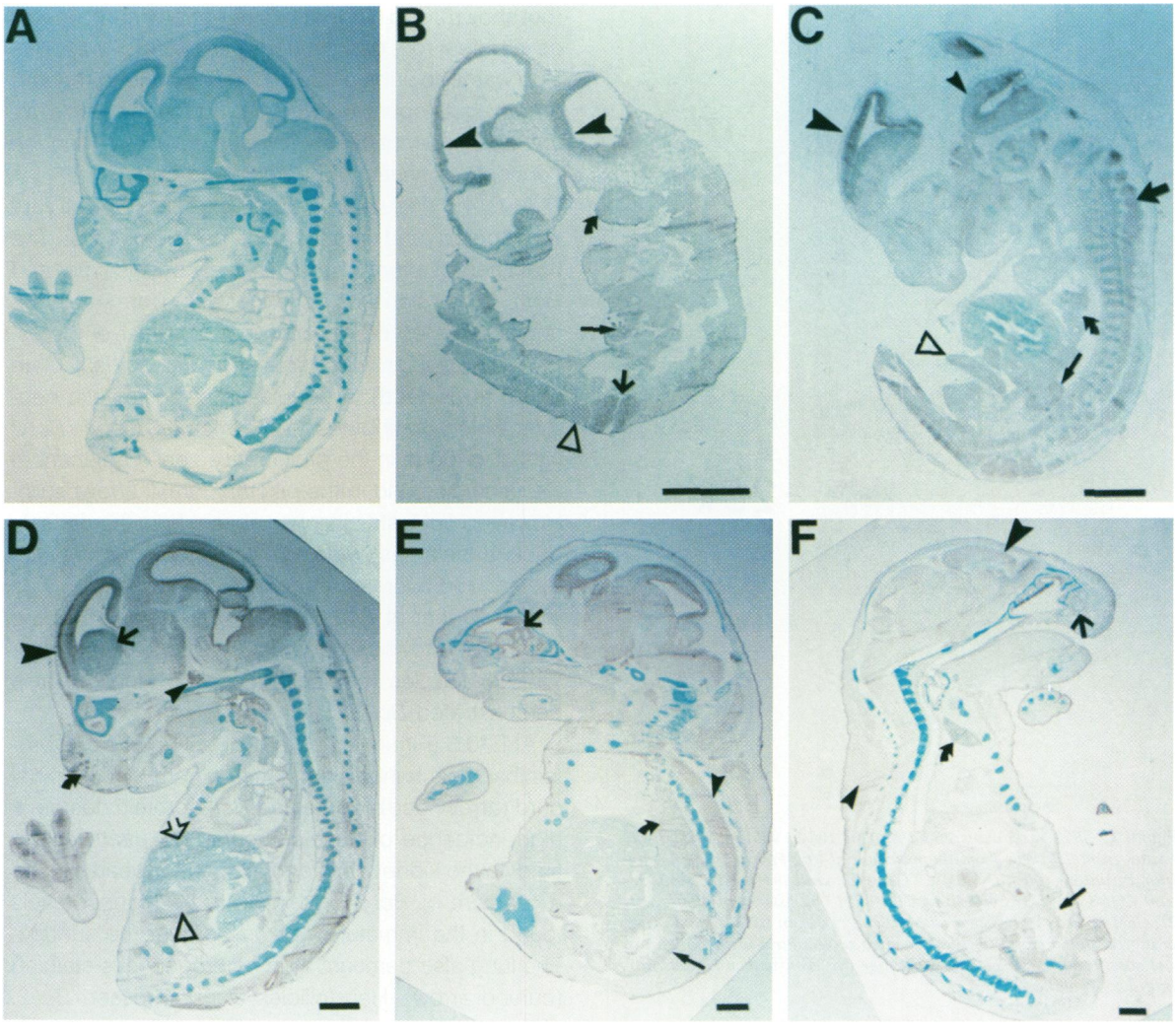

Figure 2. *Bcl-2 expression in the mouse embryo.* **A:** *Negative control section of an E14.5 mouse stained with the nonreactive hamster Ab TN3. Parasagittal sections of embryos at E10.5* (**B**), *E12.5* (**C**), *E14.5* (**D**), *E16.5* (**E**), *and E18.5* (**F**) *were stained with anti-Bcl-2 Ab 3F11. All embryo sections were stained in the same experiment and were developed identically. At E10.5* (**B**), *symbols denote neuroepithelium of the brain* (arrowhead), *spinal cord* (wide arrow), *gut* (thin arrow), *somites* (open arrowhead), *and first branchial arch* (curved arrow). *At E12.5* (**C**), *Bcl-2 was found in forebrain* (large arrowhead), *hindbrain* (small arrowhead), *and dorsal root ganglia* (large arrow). *Staining was also observed in gut* (open arrowhead), *kidney* (thin arrow), *and lung* (curved arrow). *At E14.5* (**D**), *symbols identify cortical plate* (large arrowhead), *pituitary* (small arrowhead), *and thalamus* (wide arrow). *Bcl-2 was present in whisker follicles* (curved arrow), *hindlimb, and gut* (open arrowhead), *but not in liver* (open arrow). *At E16.5* (**E**), *Bcl-2 was found in nasal epithelium* (wide arrow), *spinal cord* (arrowhead), *lung* (curved arrow), *and kidney* (thin arrow). *Surface epithelial staining was artifactual. At E18.5* (**F**), *overall levels of Bcl-2 had decreased. Cortical plate* (large arrowhead), *thymus* (curved arrow), *and tooth bud* (wide arrow) *are labeled. Staining of brown fat in the back* (small arrowhead) *and bladder* (thin arrow) *was artifactual. Scale bars = 1 mm.*

3F11 Ab (cytoplasmic and nuclear) in cells of the E16.5 cortical plate. Previous studies of *Bcl-2* in human lymphoid cell lines using confocal microscopy and subcellular fractionation demonstrated that *Bcl-2* was predominantly located within mitochondrial membranes.[14] Confocal microscopy and immunoelectron microscopy studies have also shown *Bcl-2* in endoplasmic reticulum and nuclear membranes but not within the nucleoplasm.[15,18] In Sf9 insect cells expressing *Bcl-2* from a baculovirus vector, *Bcl-2* was found in heavy membrane fractions and in nuclear fractions purified through a 2 mol/L sucrose cushion, but was not detected within the nucleus by indirect immunofluorescence.[17] To determine whether the nuclear staining we saw with 3F11 was due to the immunoperoxidase staining method, sections of cortical plate were stained with FITC-conjugated streptavidin and examined by confocal microscopy. 3F11 Ab reactivity still appeared in the cytoplasm and over the nucleus (not shown). To further elucidate the subcellular localization of *Bcl-2*, cell suspensions from E16.5 fetal brain were fractionated (Figure 3, B–E). Lysates from total brain (lane 1), sucrose purified nuclei (lane 2), heavy membrane (lane 3), light membrane (lane

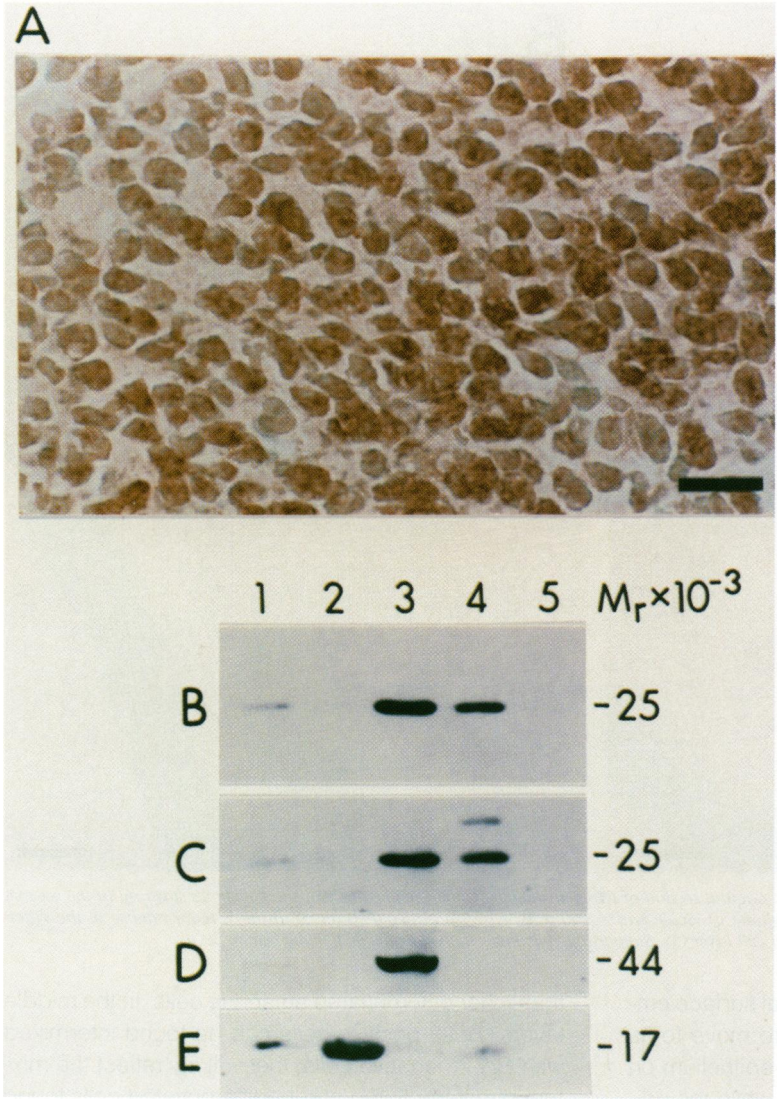

Figure 3. *Subcellular localization of Bcl-2.* **A:** *E16.5 cortical plate stained with 3F11 Ab. Scale bar = 16 μ.* **B-E:** *Cell suspensions of E16.5 brain* (**lane 1**) *were separated into nuclear* (**lane 2**), *heavy membrane* (**lane 3**), *light membrane* (**lane 4**), *and cytosol* (**lane 5**) *fractions, subjected to sodium dodecyl sulfate-polyacrylamide gel electrophoresis, and probed with anti-Bcl-2* Ab 3F11 (**B**), *anti-Bcl-2* Ab 4C11 (**C**), *anti-cytochrome b1 antiserum bc1* (**D**), *and anti-histone H3 Ab 3C1–1* (**E**). *The heavy membrane fraction contains mitochondria and lysosomes. The light membrane fraction contains plasma membranes and endoplasmic reticulum.*

4), or cytosol (lane 5) were separated by sodium dodecyl sulfate-polyacrylamide gel electrophoresis and transferred to nitrocellulose for immunoblotting. Identical lanes were probed with two independently derived Abs to m*Bcl-2*, hamster Ab 3F11 (Figure 3B) and rat Ab 4C11 (Figure 3C). These same fractions were analyzed with an antiserum to the mitochondrial marker cytochrome b1 (Figure 3D) and with an Ab to the nuclear marker histone H3 (Figure 3E). *Bcl-2* was detected in the total, heavy membrane and light membrane fractions with both anti-m*Bcl-2* Abs, but not in the nuclear fraction. The 25-kd *Bcl-2* band was the only specific product consistently recognized by the anti-*Bcl-2* Abs in lysates or in immunoblots of immunoprecipitates of up to 1 mg of these lysates (not shown). These results indicate that 3F11 recognizes the 25-kd *Bcl-2* in the fetal brain and that this protein appears to reside primarily in the heavy membrane fraction, with some protein present in the light membranes as well.

Neurosensory Epithelia

Bcl-2 expression was dramatic in the developing neurosensory epithelia of the ear, nose, and eye. Figure 4A shows a sagittal section through the ear at E18.5. *Bcl-2* expression is high in the sensory hair cells (h) and in the associated cochlear spiral ganglion (g), but is found at much lower levels in the supporting tissues.

Figure 4B shows a section through the nasal epithelium at E16.5. At this age, olfactory receptors are maturing from the stem cell population.[23] This stem

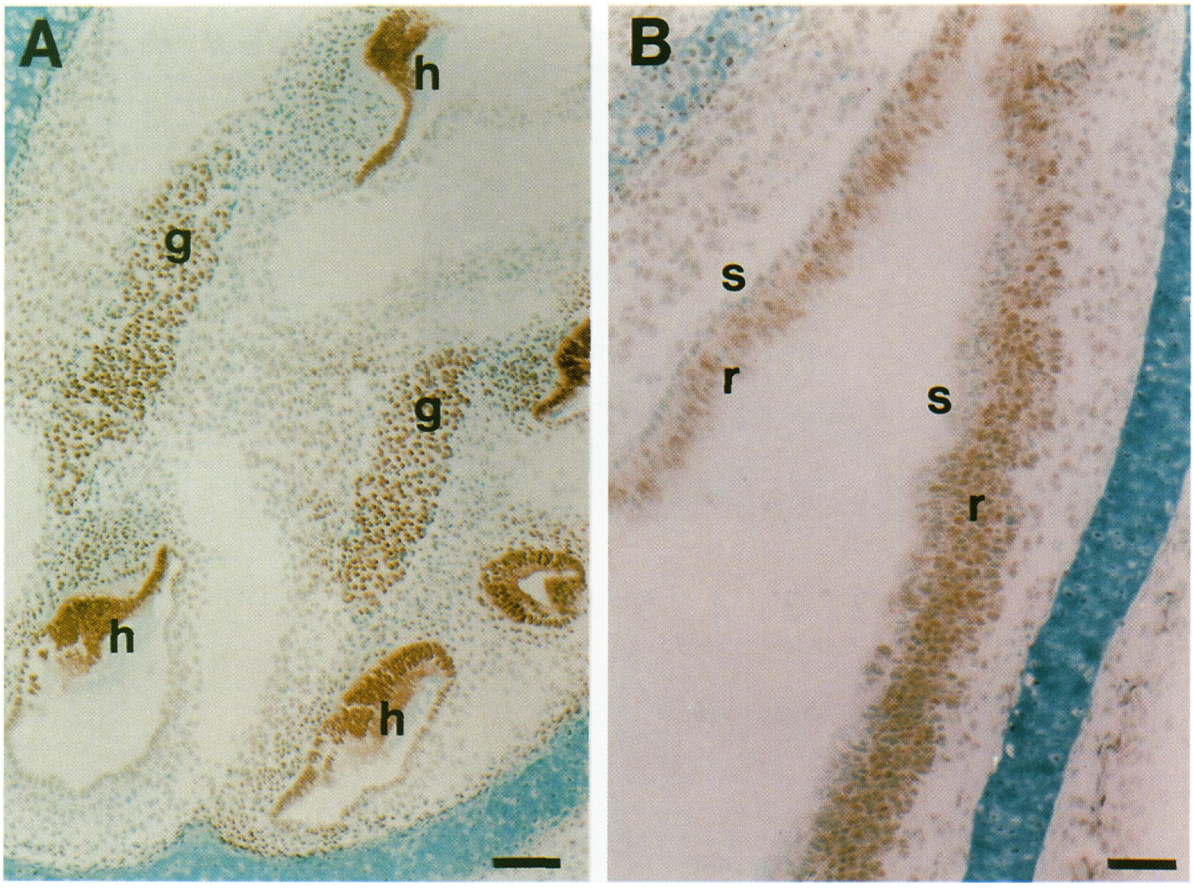

Figure 4. *Bcl-2 expression in fetal ear and nose.* **A:** *Sagittal section of E18.5 inner ear stained with 3F11 Ab. Section shows staining in the sensory hair cells (h) as well as in the cochlear spiral ganglion (g). Scale bar = 100 μ.* **B:** *E16.5 nasal epithelium. Staining is more intense in the differentiated receptors (r) than in the proliferating stem cell layer (s). Supporting cells have not yet developed. Scale bar = 50 μ.*

cell population proliferates at the luminal surface embryonically, but by E16.5 has begun to move to its adult basal location. In Figure 4B, the epithelium on the left has a basal stem cell layer (s), while the epithelium on the right has a superficial proliferating stem cell layer. *Bcl-2* is expressed at higher levels in the differentiated receptors (r) than in the stem cells. The same pattern is found in adult olfactory epithelium.[24]

Bcl-2 expression is uniformly high in the immature retina from E10.5 to E16.5, except for a few scattered cells immediately adjacent to the pigment epithelium in the mitotic zone (Figure 5A, arrow). Developing vasculature on the inside surface of the retina does not express *Bcl-2* at any time (Figure 5A, arrowhead). By E18.5, a gradient of expression becomes evident, with levels of *Bcl-2* becoming noticeably lower in cells close to the retinal pigmented epithelium (not shown). At P3 (Figure 5B) the ganglion cell layer (arrow) is separated from the rest of the retina. *Bcl-2* is expressed in all cells in the ganglion cell layer (arrow), but the remaining retina has a distinct gradient of *Bcl-2* expression, with outer undifferentiated ventricular cells containing much lower levels of *Bcl-2* protein than inner differentiated amacrine cells. In the middle layers, *Bcl-2* positive cells can be found intermixed with *Bcl-2* negative cells; these likely reflect the mixture of differentiated and undifferentiated cells found in this transitional region.

At P5 (Figure 5C), the outer plexiform layer (arrow) begins to form among differentiating photoreceptors (mostly rods in the mouse). Photoreceptors which differentiate on the inner side of the outer plexiform layer must migrate through this layer to the outer nuclear layer. *Bcl-2* expression is high in the middle layers, which will soon become the inner nuclear layer (Figure 5C, inl). However, the adjacent population of inner rods (ir) expresses low levels of *Bcl-2* similar to outer rods on the opposite side of the outer plexiform layer. Occasional horizontal cells (arrowhead) can be seen among the inner rods; these cells contain very high levels of *Bcl-2*.

At P7 (Figure 5D), there are only one or two layers of rods remaining on the inner side of the outer plexiform layer (arrow). All of the cells in the inner nuclear layer except these inner rods express high levels of *Bcl-2*. By P11 (Figure 5E), the three distinct layers

have formed with the proper constituent cells. *Bcl-2* expression is highest in ganglion cell and inner nuclear layers and lower in the outer nuclear layer. Since no more cells are generated after P11, the cellular layers thin as the eye grows to its mature size. At 3 months of age (Figure 5F), the pattern of *Bcl-2* expression in the retina is the same as at P11. Unlike many neuronal populations, retinal cells maintain *Bcl-2* expression well past the period of differentiation and cell death.

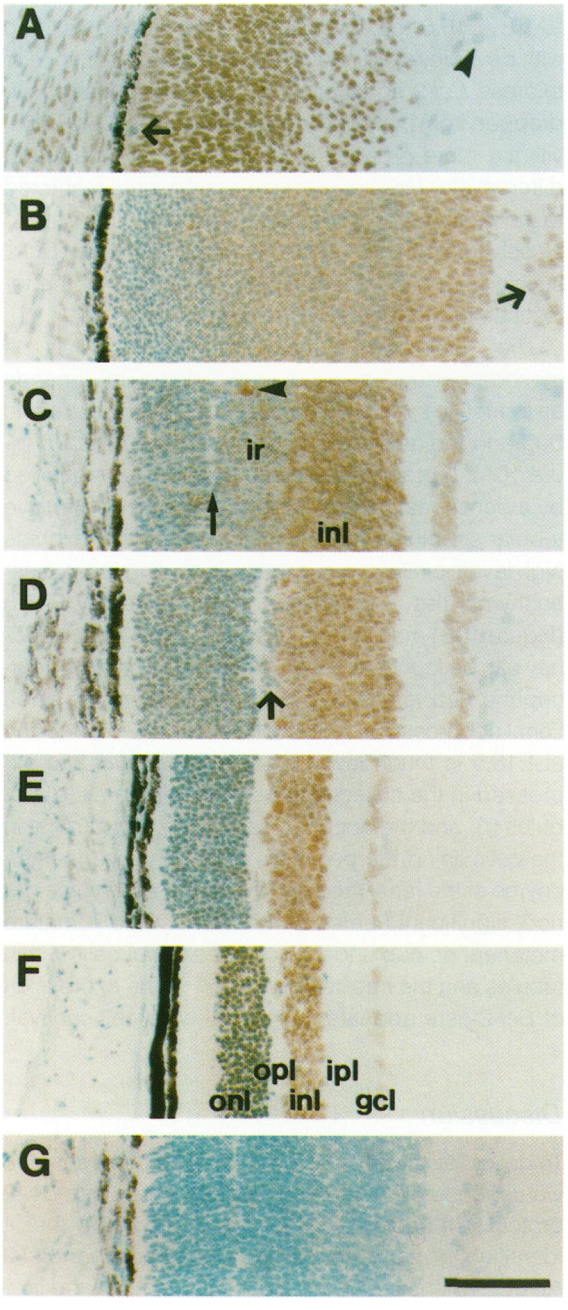

Limb Development

The limbs develop from buds consisting of a mixture of chondrogenic and myogenic cells which migrate from the somites.[25] Cells are thought to be recruited into condensations of like cell type through interactions of surface adhesion molecules, a process regulated by soluble factors.[26] Chondrogenic cells form cartilaginous templates from which the limb bones are derived. Chondrogenic cells in the interdigital zones either migrate into the digits or die *in situ*. In the developing limb, *Bcl-2* is expressed in an emerging digital pattern from E11.5 to E14.5. At E11.5 (Figure 6A), *Bcl-2* is expressed at low levels throughout the bud, with slightly increased levels in presumptive digital zones. By E12.5 (Figure 6B), aggregations of chondrogenic cells form a digital pattern; *Bcl-2* expression is high in these digital zones. Of interest, *Bcl-2* levels are lower in cells of the interdigital zone before the separation of the digits. At E13.5 (Figure 6C), *Bcl-2* expression appears to be much more restricted to the digital zones. As the digits separate at E14.5 (Figure 6D), *Bcl-2* is absent in interdigital zones but is present at high levels in precartilaginous mesenchymal condensations surrounding cartilage plates. *Bcl-2* expression is also seen at the tips of developing long bones in the limbs at this time (not shown).

Bcl-*2 Expression in Organogenesis*

The liver is derived from caudal foregut tissue at E9 and is a hematopoietic organ from E12.5 to E18.5. Hematopoietic cells in the fetal liver are susceptible to apoptosis.[27] At E14.5, *Bcl-2* is not found within parenchymal cells but is seen in hematopoietic cells within the liver (Figure 7). Megakaryocytes (arrows)

Figure 5. *Changes in Bcl-2 expression in the developing retina. Sections A to F stained with 3F11, section G stained with TN3.* **A:** *E16.5 retina shows uniform staining in the neuroepithelium except for scattered cells adjacent to the pigment epithelium* (arrow). *Endothelial cells along the inner aspect are denoted with an arrowhead.* **B:** *P3 retina shows a gradient of staining from the pigment epithelium to the ganglion cell layer* (arrow). **C:** *P5 retina shows a well-defined inner plexiform layer separating the ganglion cell layer from the ventricular stratum and the beginnings of an outer plexiform layer* (arrow) *within the differentiating rods, creating a population of inner rods* (*ir*). *Bcl-2 expression is high in the ganglion cell layer and the inner third of the ventricular stratum which becomes the inner nuclear layer* (*inl*). *Large cells near the outer plexiform layer which stain strongly for Bcl-2 are horizontal cells* (arrowhead). **D:** *P7 retina shows a well developed outer plexiform layer with a few rods remaining on the inner side* (arrow). **E:** *P11 retina shows the basic adult structure of the retina.* **F:** *3-month retina shows the outer nuclear layer* (*onl*), *inner nuclear layer* (*inl*), *ganglion cell layer* (*gcl*), *outer plexiform layer* (*opl*), *and inner plexiform layer* (*ipl*). **G:** *Negative control section of P5 retina shows very little background staining with the TN3 Ab. Scale bar* (*A–G*) = 100 μ.

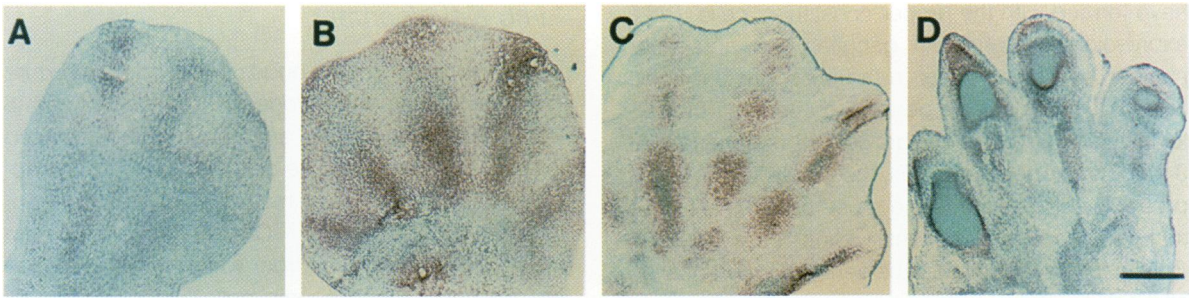

Figure 6. *Bcl-2 expression in the developing forelimb.* **A:** *E11.5 limb shows light staining in presumptive digital regions.* **B:** *E12.5 limb demonstrates very strong staining in the digital regions and in the apical ectodermal ridge and weak staining in the interdigital zones.* **C:** *E13.5 limb shows strong staining in the digits and little or no staining in the apical ectodermal ridge and interdigital zones.* **D:** *E14.5 limb has cartilage plates surrounded by precartilagenous condensations which stain strongly with 3F11. Scale bar = 250 μ.*

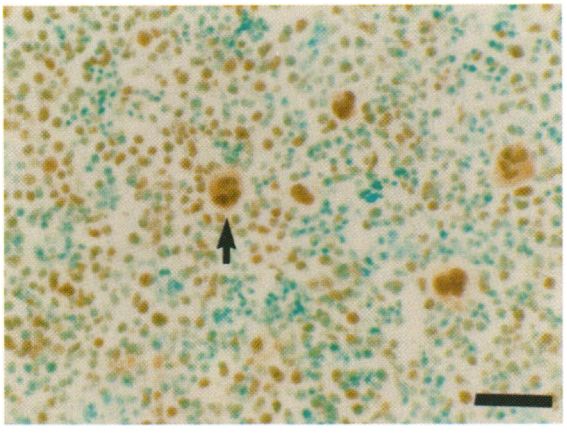

Figure 7. *Bcl-2 is expressed in hematopoietic cells in the developing liver. E14.5 liver shows staining in hematopoietic cells, especially megakaryocytes* (**arrow**), *but not in liver parenchymal cells. Scale bar = 50 μ.*

which express high levels of *Bcl-2* can easily be identified in this section. Although the liver has a high regenerative potential in adult life, *Bcl-2* is not expressed in liver parenchymal cells in the developing liver at any time nor in the normal adult liver (not shown).

The epithelium of the bronchial tree is derived from a budding of the foregut at E10. The lung bud branches repeatedly to give rise to right and left lungs and then to successive levels of the bronchial tree. At E12.5 (Figure 8A), *Bcl-2* expression is higher in the thicker more proximal region of the lung bud (p) than in the thinner distal epithelium (d). This proximal-distal gradient of expression is maintained as cells within the lung differentiate. By E18.5 (Figure 8B), the lung is composed of a large number of blood vessels (v) as well as branching airways (a) leading to functional alveoli. *Bcl-2* is expressed at high levels in the bronchiolar cells of the airways but at much lower levels in the alveoli and blood vessels.

The epithelium of the small intestine is derived from the midgut. At E14.5, the epithelium is undifferentiated and all cells express high levels of *Bcl-2* (Figure 9A). By E16.5, the epithelium has become convoluted with developing villi, but all epithelial cells continue to express *Bcl-2* equally, although the level may have dropped from that seen at E14.5 (Figure 9B). At E18.5, villi are more pronounced and cells have begun to differentiate; *Bcl-2* expression has become restricted to the base of the villi (Figure 9C, arrow). This pattern closely resembles that seen in the adult in which *Bcl-2* staining is only present in the cells found in the intestinal crypts (Figure 9D, arrow).

The definitive kidney (metanephros) is a mesoderm-derived tissue; its development depends on inductive events which occur between the ureteric bud and the metanephric mesoderm. At E12.5 (Figure 10A), a branched ureteric bud (u) is surrounded by a dense metanephric cap (m) and some primitive tubular structures (t). All of these structures express high levels of *Bcl-2*, while the surrounding loose mesenchymal tissue expresses lower levels. By E16.5 (Figure 10B) many of the elements of the mature kidney can be found, although the undifferentiated metanephric cap is still present and will generate additional nephrons. Overall, the level of *Bcl-2* expression at E16.5 is much lower than at E12.5. *Bcl-2* is expressed in the collecting ducts (c), glomeruli (g), tubules (t), and metanephric cap tissue (m), but not in the cells lining the pelvis (p) or in the loose mesenchyme of the renal medulla. In the late embryonic period, significant numbers of cells near the immature metanephric cap undergo cell death, but cells within tubules and the cap itself do not.[28,29] The expression of *Bcl-2* here appears to correlate with cell survival.

Discussion

To delineate the expression of *Bcl-2* in development, we used the 3F11 Ab monospecific for mouse *Bcl-2* protein. Characterization of this Ab showed that it identified the same cell types as the anti-human *Bcl-2* Ab 6C8 when used in immunohistochemical and flow

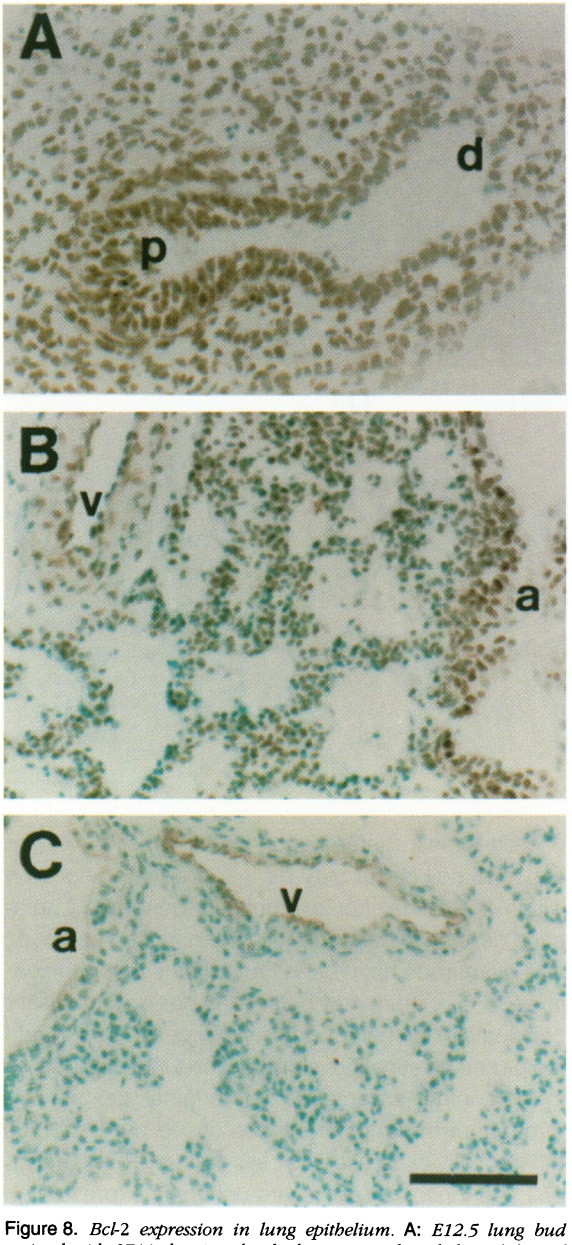

Figure 8. *Bcl-2 expression in lung epithelium.* **A:** *E12.5 lung bud stained with 3F11 showing the thicker proximal epithelium (p) and thinner distal epithelium (d).* **B:** *Section of E18.5 lung contains proximal airways (a) and alveoli and blood vessels (v).* **C:** *Negative control section of E18.5 lung stained with TN3. Scale bar = 100 μ.*

cytometric analysis of adult thymus.[10,11] In addition, in the few tissues which the rat anti-mouse *Bcl-2* Ab will stain *in situ* (eg, dorsal root ganglia), 3F11 and 4C11 identify the same cell types.[24] However, while the 6C8 and 4C11 monoclonal Abs consistently show a cytoplasmic staining pattern when used on frozen tissue sections, 3F11 stains the nucleus as well as the cytoplasm in many cell types. Another anti-human *Bcl-2* Ab[30] has shown staining of mitochondria, endoplasmic reticulum, and outer nuclear membrane or perinuclear membrane.[15,18] To further address the localization of *Bcl-2*, we performed subcellular fractionation of mouse fetal brain. In these experiments, *Bcl-2* (as recognized by 3F11 and 4C11) co-localized primarily with heavy membranes possessing mitochondrial markers and with light membranes containing endoplasmic reticulum and not with nuclei. It is possible that the nuclear-associated membranes which have been shown in some studies to contain *Bcl-2* may have been removed by our sucrose gradient centrifugation.

During embryogenesis, *Bcl-2* could be found in derivatives of all three germ layers; however, this expression was not ubiquitous. Ectodermal derivatives that contained *Bcl-2* included cells of the central nervous system and peripheral nervous system, retina, otic and nasal epithelia, and epidermis. Mesodermal tissues expressing *Bcl-2* included chondrocytes, kidney, and tongue muscle. Lung and intestine, endoderm-derived tissues, also expressed *Bcl-2*. *Bcl-2* was not found in loose connective tissue zones, liver parenchymal cells, or in nucleated red blood cells.

Bcl-2 protein was found at the earliest time point examined, E8.5, throughout the neuroepithelium. In fact, *Bcl-2* was abundantly expressed in neuronal tissues throughout gestation. The details of neural expression are described elsewhere.[24] As organogenesis proceeds, *Bcl-2* is expressed in various anlage. At E10.5, *Bcl-2* was found in the eye, gut, and metanephric tissues, as well as in neuroectoderm. By E12.5, *Bcl-2* could also be identified in the lung and mesonephros. In general, *Bcl-2* was expressed in all well-formed structures at E12.5 except the liver parenchyma. During organ differentiation, *Bcl-2* expression became increasingly restricted to certain cell types within each tissue. For example, *Bcl-2* was expressed throughout the undifferentiated intestinal epithelium but was restricted to the zones of progenitors as cells within the villi matured.

In some tissues the pattern of *Bcl-2* expression correlates with periods of developmental cell death. In the limb of the mouse, the most prominent regions of cell death are the interdigital necrotic zones. *Bcl-2* is expressed at high levels in digital zones at E11.5 to 14.5 and at decreasing levels in interdigital zones through this period. *Bcl-2* expression at E14.5 and later is particularly high in precartilaginous condensations surrounding mature cartilage. Expression of high levels of *Bcl-2* in the chondrocytes which form the digits may be an important factor in their survival. Cells in the interdigital zones do not express *Bcl-2* and may therefore be susceptible to signals for cell death. Regression of cells within interdigital necrotic zones is dependent upon epithelial-mesenchymal in-

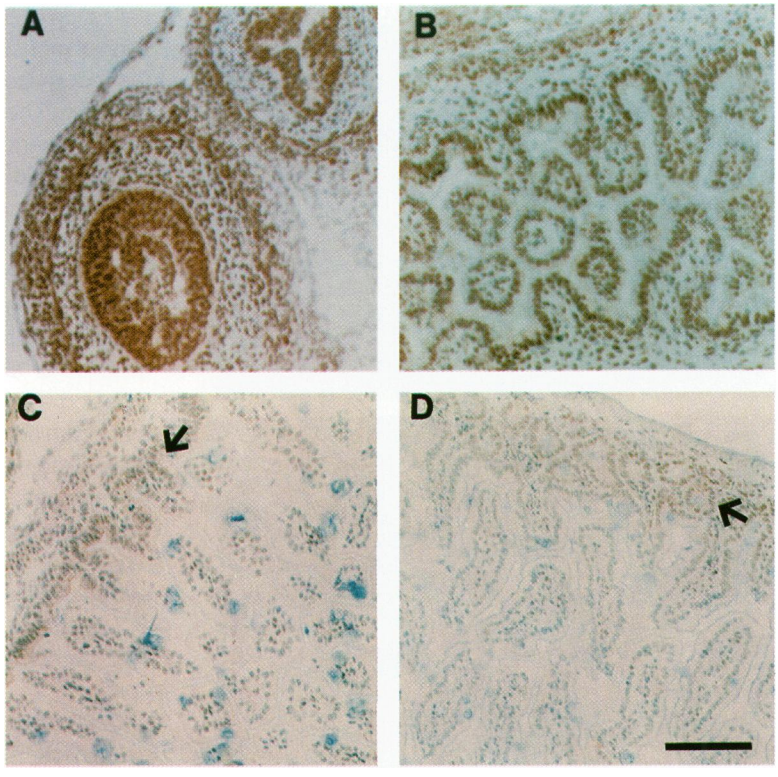

Figure 9. *Bcl-2 protein becomes regionally restricted as the intestinal epithelium matures.* **A:** *E14.5 gut has high levels of Bcl-2 in the epithelial and outer muscular layers.* **B:** *E16.5 gut shows Bcl-2 staining throughout the epithelial layer.* **C:** *E18.5 intestine expresses Bcl-2 only at the base of the villi* (**arrow**). **D:** *3-month small intestine shows Bcl-2 staining only in crypts and lower villi* (**arrow**). *Overall intensity of Bcl-2 staining decreases with age. Scale bar = 100 μ.*

teractions through the basal lamina which separates these tissues. Normally, the basal lamina degenerates and the underlying mesenchyme dies.[31] When the interaction between the interdigital mesenchyme and its overlying dorsal or apical ectoderm is disrupted, death is decreased and ectopic chondrogenesis occurs.[32,33] These observations suggest that the mesenchyme is pre-programmed for chondrogenesis but can be induced to die via interactions with the overlying ectoderm. Down-regulation of *Bcl-2* in the interdigital regions may be important for the induction of interdigital cell death to occur. However, *Bcl-2*-deficient mice have grossly normal limbs, arguing that *Bcl-2* expression is not solely required for the maintenance of digital architecture.

Bcl-2 expression was examined in detail in the postnatal retina because cell death in this organ has been well documented. Cell death occurs in all retinal cell types and approximately coincides with the period of migration and synapse formation represented by the appearance of the plexiform layers.[34–37] However, the exact timing and extent of death differs among the layers and occurs in a centroperipheral gradient. Target cell competition has been suggested as one cause of cell death in the retina. In the human, cell loss in the ganglion cell layer coincides with axon loss in the optic nerve.[36] In the rat, contralateral enucleation or optic tract lesion increases the number of cells in the ipsilateral ganglion cell layer.[38] Another cause of cell death may be inappropriate migration within the retina. For example, degenerating amacrine cells have been found in the ganglion cell layer, and dying rods have been found in the inner nuclear layer.[34,35,37] There may be several distinct signals for cell death in the retina. *Bcl-2* is expressed throughout the period of retinal development and into maturity. As in many other organs, *Bcl-2* is originally expressed throughout the undifferentiated tissue but becomes differentially expressed as cells mature. The ganglion cell and inner nuclear layers uniformly express high levels of *Bcl-2*, while most cells in the outer nuclear layer express lower levels. These relative levels seem to be established as soon as cells differentiate and in the same centroperipheral gradient. Interestingly, along with their lower expression of *Bcl-2*, photoreceptors seem to have a lower rate of developmental cell death than other retinal cells.[39] Because of this, there may be less pressure to retain *Bcl-2* expression. However, in retinitis pigmentosa, a retinal degeneration caused by several gene defects, photoreceptors are progressively lost, suggesting that photoreceptors are susceptible to death. Mouse models of three of these defects show apoptotic death of photoreceptor cells.[39] Perhaps the low level of *Bcl-2* makes photoreceptors susceptible to death in the presence of genetic imbalances.

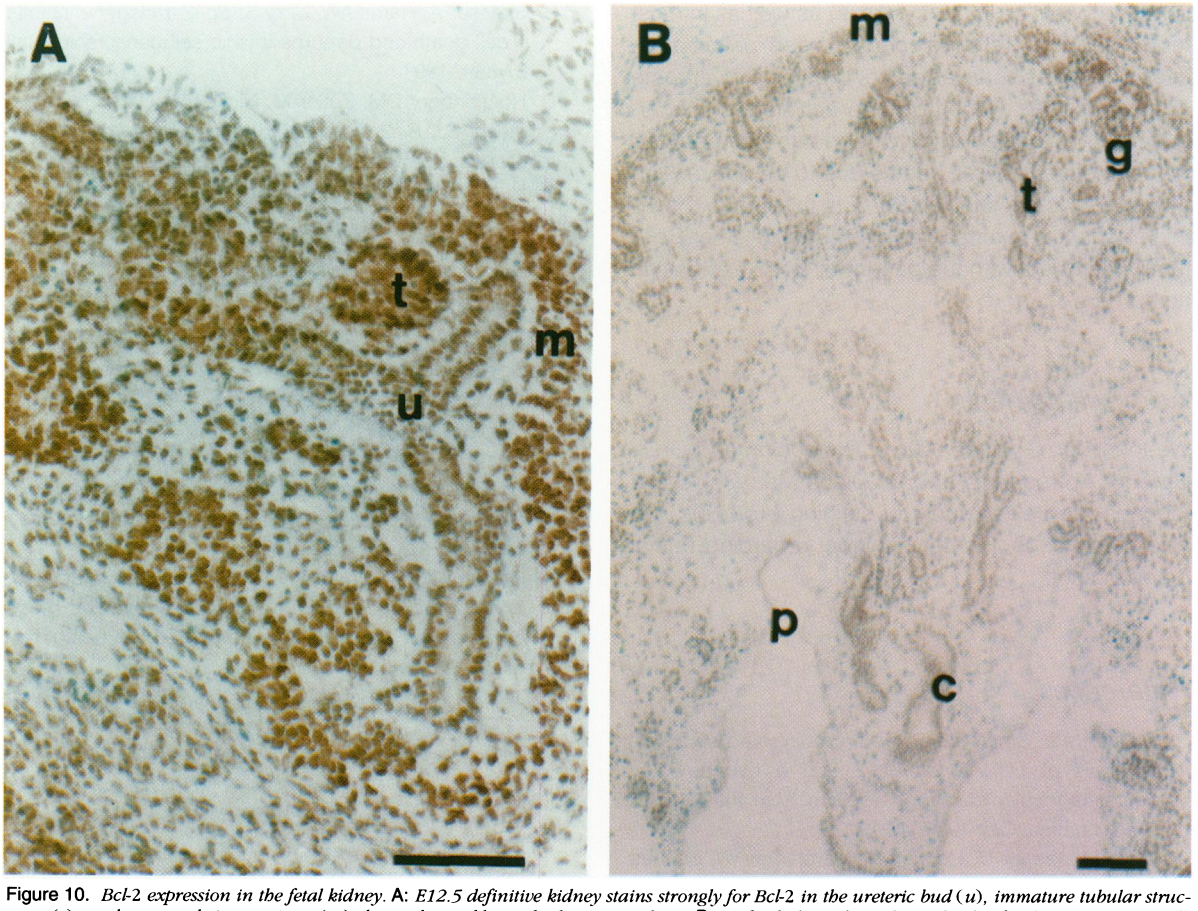

Figure 10. *Bcl-2 expression in the fetal kidney.* **A:** *E12.5 definitive kidney stains strongly for Bcl-2 in the ureteric bud (u), immature tubular structures (t), and metanephric cap tissue (m), but only weakly in the loose mesoderm.* **B:** *E16.5 kidney shows lower levels of Bcl-2 staining overall. Bcl-2 protein remains in metanephric cap tissue (m), glomeruli (g), tubules (t), and collecting ducts (c), but is not found in the epithelium lining the renal pelvis (p) or in the loose mesenchyme of the medulla. Scale bars = 100 μ.*

The kidney is another organ in which cell death is a prominent feature of development. Apoptosis occurs in mesenchyme-derived cells in islands between developing nephrons in the nephrogenic zone and in cells of the distal renal papilla, which may be derived from the ureteric bud.[28,29] However, cell death is not observed in the undifferentiated metanephric cap or in the tubules themselves. Mesenchymal cells are induced to become epithelial tubule cells by the ureteric bud; in turn, the ureteric bud is induced to branch by the mesenchyme.[40] Among mesenchymal cells, the pattern of cell death is consistent with initiation of induction followed by insufficient growth factor availability. In support of this hypothesis, administration of epidermal growth factor *in vitro* and *in vivo* greatly reduced the incidence of cell death.[28,29] How does the expression of *Bcl-2* fit into this scheme of kidney development? From E12.5 to E16.5, *Bcl-2* was found at high levels in undifferentiated cap tissue, ureteric bud, and nephron structures, correlating well with the lack of cell death in these structures. In the *Bcl-2* –/– mice, kidneys are small and underdeveloped by E12.5 (C. Sorenson and S. J. Korsmeyer, in press) and progress to polycystic kidney disease.[13] Therefore, this pattern of *Bcl-2* expression is important in kidney development, perhaps in the inductive relationship between the metanephric cap and ureteric bud which dictates differentiation and cell survival.

Despite the widespread expression of *Bcl-2* in normal embryos, most organs with the exception of the kidney display relatively normal development in *Bcl-2*-deficient mice. This is perhaps surprising, as *Bcl-2* is a central repressor of an evolutionarily conserved death pathway common to multicellular organisms. *Bcl-2* can even substitute for its homologue, ced-9, in the nematode *Caenorhabditis elegans.*[41,42] One possible explanation for the viability of *Bcl-2*-deficient mice relates to an emerging family of *Bcl-2*-related molecules which might provide a redundancy in death repressor activity during embryogenesis.[43–45]

Bcl-2 expression in many progenitor-type cells of the adult (such as the crypt cells of intestinal epithe-

lium and basal cells of epidermis) as well as in most fetal tissues may reflect a common need for immature cells to express survival factors in order to overcome a stage-specific vulnerability to cell death. This argues that the susceptibility to cell death may be wider than the observed cell deaths due to the expression of survival factors such as *Bcl-2*. In this context, it will be important to compare the expression of other *Bcl-2* family members with the pattern of *Bcl-2* expression noted here.

Acknowledgments

We thank Dr. G. Nuñez, Dr. J. Portanova, and Dr. J. Hare for Ab reagents and Dr. Diane Merry for assistance in the development of staining protocols. We also thank Dr. D. Fox for his input regarding retinal development.

References

1. Cleary M L, Smith SD, Sklar J: Cloning and structural analysis of cDNAs for *Bcl-2* and a hybrid *Bcl-2*/immunolgobulin transcript resulting from the t(14;18) translocation. Cell 1986, 47:19–28
2. Seto M, Jaeger U, Hockett RD, Graninger W, Bennett S, Goldman P, Korsmeyer SJ: Alternative promoters and exons, somatic mutation and transcriptional deregulation of the *Bcl-2*-Ig fusion gene in lymphoma. EMBO J 1988, 7:123–131
3. Graninger WB, Seto M, Boutain B, Goldman P, Korsmeyer SJ: Expression of *Bcl-2* and *Bcl-2*-Ig fusion transcripts in normal and neoplastic cells. J Clin Invest 1987, 80:1512–1515
4. McDonnell TJ, Korsmeyer SJ: Progression from lymphoid hyperplasia to high-grade malignant lymphoma in mice transgenic for the t(14;18). Nature 1991, 349: 254–256
5. McDonnell TJ, Nuñez G, Platt FM, Hockenbery D, London L, McKearn JP, Korsmeyer SJ: Deregulated *Bcl-2*-immunoglobulin transgene expands a resting but responsive immunoglobulin M and D-expressing B-cell population. Mol Cell Biol 1990, 10:1901–1907
6. Nuñez G, London L, Hockenbery D, Alexander M, McKearn JP, Korsmeyer SJ: Deregulated *Bcl-2* gene expression selectively prolongs survival of growth factor-deprived hemopoietic cell lines. J Immunol 1990, 144:3602–3610
7. Vaux DL, Cory S, Adams JM: *Bcl-2* gene promotes haemopoietic cell survival and cooperates with c-myc to immortalize pre-B cells. Nature 1988, 335:440–442
8. Sentman CL, Shutter JR, Hockenbery D, Kanagawa O, Korsmeyer SJ: *Bcl-2* inhibits multiple forms of apoptosis but not negative selection in thymocytes. Cell 1991, 67:879–888
9. Strasser A, Harris AW, Cory S: *Bcl-2* transgene inhibits T cell death and perturbs thymic self-censorship. Cell 67:889, 1991
10. Hockenbery DM, Zutter M, Hickey W, Nahm M, Korsmeyer SJ: *Bcl2* protein is topographically restricted in tissues characterized by apoptotic cell death. Proc Natl Acad Sci USA 1991, 88:6961–6965
11. Veis DJ, Sentman CL, Bach EA, Korsmeyer SJ: Expression of the *Bcl-2* protein in murine and human thymocytes and in peripheral T lymphocytes. J Immunol 1993, 151:2546–2554
12. Merino R, Ding L, Veis DJ, Korsmeyer SJ, Nuñez G: Developmental regulation of the *Bcl-2* protein and susceptibility to cell death in B lymphocytes. EMBO J 1994, 13:683–691
13. Veis DJ, Sorenson CM, Shutter JR, Korsmeyer SJ: *Bcl-2* deficient mice demonstrate fulminant lymphoid apoptosis, polycystic kidneys, and hypopigmented hair. Cell 1993, 75:229–240
14. Hockenbery D, Nunez G, Milliman C, Schreiber RD, Korsmeyer SJ: *Bcl-2* is an inner mitochondrial membrane protein that blocks programmed cell death. Nature 1990, 248:334–336
15. Jacobson MD, Burne JF, King MP, Miyashita T, Reed JC, Raff MC: *Bcl-2* blocks apoptosis in cells lacking mitochondrial DNA. Nature 1993, 361:365–369
16. Chen-Levy Z, Nourse J, Cleary MJ: The *Bcl-2* candidate proto-oncogene product is a 24-kilodalton integral-membrane protein highly expressed in lymphoid cell lines and lymphomas carrying the t(14;18) translocation. Mol Cell Biol 1989, 9:701–710
17. Alnemri ES, Robertson NM, Fernandes TF, Croce CM, Litwack G: Overexpressed full-length human *Bcl2* extends the survival of baculovirus-infected Sf9 insect cells. Proc Natl Acad Sci USA 1992, 89:7295–7299
18. Monaghan P, Robertson D, Amos TAS, Dyer MJS, Mason DY, Greaves MF: Ultrastructural localization of *Bcl-2* protein. J Histochem Cytochem 1992, 40:1819–1825
19. Hockenbery DM, Oltvai ZN, Yin X-M, Milliman CL, Korsmeyer SJ: *Bcl-2* functions in an anti-oxidant pathway to prevent apoptosis. Cell 1993, 75:241–251
20. Kane DJ, Sarafian TA, Anton R, Hahn H, Gralla EB, Valentine JS, Ord T, Bredesen DE: *Bcl-2* inhibition of neural death: decreased generation of reactive oxygen species. Science 1993, 262:1274–1277
21. Glucksmann A: Cell deaths in normal vertabrate ontogeny. Biol Rev 1951, 26:59–86
22. LeBrun DP, Warnke RA, and Cleary ML: Expression of *Bcl-2* in fetal tissues suggests a role in morphogenesis. Am J Pathol 1993, 142:743–753
23. Brujnes PC, Frazier LL: Maturation and plasticity in the olfactory system of vertebrates. Brain Res Rev 19876, 11:1–45
24. Merry DE, Veis DJ, Hickey WF, Korsmeyer SJ: *Bcl-2* protein expression is widespread in the developing nervous system and retained in the adult PNS. Development 1994, 120:301–311

25. Michaelson J: Cell selection in development. Biol Rev 1987, 62:115–139
26. Jiang T-X, Yi J-R, Ying S-Y, Chuong C-M: Activin enhances chondrogenesis of limb bud cells: stimulation of precartilaginous mesenchymal condensations and expression of NCAM. Dev Biol 1993, 155:545–557.
27. Yu H, Bauer B, Lipke GK, Phillips RL, Van Zant G: Apoptosis and hematopoiesis in murine fetal liver. Blood 1993, 81:373–384
28. Coles HSR, Burne JF, Raff MC: Large-scale normal cell death in the developing rat kidney and its reduction by epidermal growth factor. Development 1993, 118:777–784
29. Koseki C, Herzlinger D, Al-Awqati Q: Apoptosis in metanephric development. J Cell Biol 1993, 119: 1327–33
30. Pezzella F, Tse AGD, Cordell JL, Pulford KAF, Gatter KC, Mason DY: Expression of the *Bcl-2* oncogene protein is not specific for the 14;18 chromosomal translocation. Am J Pathol 1990, 137:225–232
31. Hurle JM, Fernandez-Teran MA: Fine structure of the regressing interdigital membranes during the formation of the digits of the chick embryo leg bud. J Embryol Exp Morphol 1983, 78:195–209
32. Hurle JM, Fernandez-Teran MA: Fine structure of the interdigital membranes during the morphogenesis of the digits of the webbed foot of the duck embryo. J Embryol Exp Morphol 1984, 79:201–210
33. Hurle JM, Gañan Y: Interdigital tissue chondrogenesis induced by surgical removal of the ectoderm in the embryonic chick leg bud. J Embryol Exp Morphol 1986, 94:231–244
34. Spira A, Hudy S, Hannah R: Ectopic photoreceptor cells and cell death in the developing rat retina. Anat Embryol 1984, 169:293–301.
35. Young RW: Cell death during differentiation of the retina in the mouse. J Comp Neurol 1984, 229:362–373
36. Provis JM: Patterns of cell death in the ganglion cell layer of the human fetal retina. J Comp Neurol 1987, 259:237–246
37. Robinson SR: Cell death in the inner and outer nuclear layers of the developing cat retina. J Comp Neurol 1988, 267:507–515
38. Linden R, Serfaty CA: Evidence for differential effects of terminal and dendritic competition upon developmental neuronal death in the retina. Neuroscience 1985, 15:853–868
39. Chang G-Q, Hao Y, Wong F: Apoptosis: final common pathway of photoreceptor death in rd, rds, and rhodopsin mutant mice. Neuron 1993, 11:595–605
40. Saxen L, Sariola H: Early organogenesis of the kidney. Pediatr Nephrol 1987, 1:385–392
41. Vaux DL, Weissman IL, Kim SK: Prevention of programmed cell death in *Caenorhabditis elegans* by human *Bcl-2*. Science 1992, 258:1955–1957
42. Hengartner MO, Horvitz HR: C. elegans cell survival gene ced-9 encodes a functional homolog of the mammalian proto-oncogene *Bcl-2*. Cell (in press)
43. Kozopas KM, Yang T, Buchan HL, Zhou P, Craig RW: MCL-1, a gene expressed in programmed myeloid cell differentiation, has sequence similarity to *Bcl-2*. Proc Natl Acad Sci USA 1993, 90:3516–3520
44. Boise LH, Gonzalez-Garcia M, Postems CE, Ding L, Lindsten T, Turka LA, Mao X, Nunez G, Thompson CB: *Bcl-x*, a *Bcl-2* related gene that functions as a dominant regulator of apoptotic cell death. Cell 1993, 74: 597–608
45. Lin EY, Orlofsky A, Berger MS, Prystowsky MD: Characterization of A1, a novel hemopoietic-specific early-response gene with sequence similarity to *Bcl-2*. J Immunol 1993, 151:1979–1988